DOI: http://dx.doi.org/10.12989/sem.2007.25.1.053

# An effective load increment method for multi modal adaptive pushover analysis of buildings

K. Türker† and E. İrtem‡

*Balıkesir University, Civil Engineering Department, 10145 Balıkesir, Turkey*

*(Received December 23, 2005, Accepted August 17, 2006)*

**Abstract.** In this study, an effective load increment method for multi modal adaptive non-linear static (pushover) analysis (NSA) for building type structures is presented. In the method, lumped plastisicity approach is adopted and geometrical non-linearties (second-order effects) are included. Non-linear yield conditions of column elements and geometrical non-linearity effects between successive plastic sections are linearized. Thus, load increment needed for formation of plastic sections can be determined directly (without applying iteration or step-by-step techniques) by using linearized yield conditions. After formation of each plastic section, the higher mode effects are considered by utilizing the essentials of traditional response spectrum analysis at linearized regions between plastic sections. Changing dynamic properties due to plastification in the system are used on the calculation of modal lateral loads. Thus, the effects of stiffness changes and local mechanism at the system on lateral load distribution are included. By using the proposed method, solution can be obtained effectively for multi-mode whereby the properties change due to plastifications in the system. In the study, a new procedure for determination of modal lateral loads is also proposed. In order to evaluate the proposed method, a 20 story RC frame building is analyzed and compared with Non-linear Dynamic Analysis (NDA) results and FEMA 356 Non-linear Static Analysis (NSA) procedures using fixed loads distributions (first mode, SRSS and uniform distribution) in terms of different parameters. Second-order effects on response quantities and periods are also investigated. When the NDA results are taken as reference, it is seen that proposed method yield generally better results than all FEMA 356 procedures for all investigated response quantities.

**Keywords:** earthquake response of buildings; load increment method; adaptive non-linear static analysis; second-order effects; RC buildings.

## 1. Introduction

Today, seismic behavior (local and global mechanism, force and deformation demands of elements etc.) of low-rise buildings without structural irregularities can be determined more accurately by non-linear static analysis (NSA) procedures. In these buildings, it can be assumed that, the first (fundamental) mode is the most effective one in the structural behavior and this effectiveness do not change due to formation of the plastification (plastic hinging with bending and axial deformations). Therefore, traditional non-linear static analysis (T-NSA) procedures which is based on monotonically increasing lateral loads proportional to the first mode or similar shapes yield

† Research Assistant, Ph.D., Corresponding author, E-mail: kturker@balikesir.edu.tr
‡ Associate Professor, Ph.D., E-mail: eirtem@balikesir.edu.tr

sufficiently good products. However, investigations on low-rise irregular buildings, as well as high-rise regular or irregular buildings show that the T-NSA procedures are not sufficient in determination of the non-linear seismic behavior (Lawson *et al.* 1994, Kim and D'Amore 1999, Mwafy and Elnashai 2001, FEMA 440 2004). In these buildings, higher modes besides fundamental modes are effective in structural behavior and/or modal properties of the buildings change extremely due to plastification in system. Therefore, higher mode effects and/or change of dynamic properties due to plastification in system should be considered in NSA applied to these buildings. Recently, improved pushover procedures including multi-mode and/or effect of plastification in system on mode shapes (adaptive procedures) have been developed by several researchers in order to overcome the deficiencies of T-NSA procedures (Paret *et al.* 1996, Yang and Wang 1998, Moghadam 1998, Gupta and Kunnath 2000, Elnashai 2001, Chopra and Goel 2001, Chopra and Goel 2002, Antoniou *et al.* 2002, Aydınoglu 2003, Jan *et al.* 2004, Montes *et al.* 2004, Goel and Chopra 2005, Aschheim and Hernandez-Montes 2006). Generally, load increment methods based on iterative approximations or step-by-step solution approaches are used in the modal and adaptive analysis procedures. In these procedures, determination of formation of plastic sections and change of dynamic properties increase computation process to a large extent. Furthermore, some mathematical stability problem can arise in application of changing load distribution along the building height due to formation of plastic section (Rovitakis 2001, Elnashai 2001). For these reasons, development of more effective methods is needed for non-linear analysis of buildings. In the study, an effective load increment method is presented for multi-mode and adaptive non-linear static analysis of buildings. In order to evaluate the proposed method, a 20 story RC frame building is analyzed by using the method. The results are then compared with results of NSA performed for three fixed load distributions (first mode, SRSS, uniform) in FEMA 356 (2000), and non-linear dynamic analysis (NDA) in terms of different parameters. By using the proposed method, non-linear seismic response of buildings affected by higher modes can be effectively determined for many modes changing due to plastification in system.

## 2. Description of load increment method

### 2.1 Assumptions

The scope of this study is restricted to plane frame systems. However, essentials of the proposed method are general and it can be applied to 3D systems readily. Internal force-deformation relationships of elements subjected to pure bending moment or bending moment combined with axial force are assumed as elastic-perfectly plastic behavior. Lumped plasticity approach is adopted for bending and axial deformations. Yield conditions of elements depend only on bending moment and/or axial force and the effect of shear forces is neglected. Yield vector is assumed to be normal to the yield curve for elements subjected to bending moment combined with axial force. Second order effects are included for column elements and neglected for beam elements that have negligible axial forces.

### 2.2 Principals of the proposed method

The method is based on linerization of geometrical non-linearity effects between successive plastic sections and yield conditions of column elements. The effects of higher modes are considered by utilizing the essentials of traditional response spectrum analysis in the linearized regions between successive plastic sections.

#### *2.2.1 Linearization of geometrical non-linearity effects (second-order effects)*

Seismic behavior of buildings is generally determined for constant gravity loads composed of dead and live loads since the probability of change of gravity loads is small. Therefore, second order effects can be considered by including the axial forces resulting from gravity loads in stability functions of elements. Thus, geometrical non-linearity effects between formations of successive plastic sections are linearized in the solution of system. It is well known that axial force values of columns in lower stories of high-rise buildings vary extremely due to increasing lateral loads. In this case, the solution of system should be repeated for axial force values obtained in the last step of the analysis. However, effect of the change of axial forces can be neglected since the sum of the axial forces of columns at any story does not change (Irtem 1991). Therefore, repetition of the solution is generally not required in building type structures.

#### *2.2.2 Yield conditions and linearization of yield conditions (interaction diagrams)*

In ductile structures, when the internal forces in any section reach to the critical values defined by the yield (failure) condition, a plastic section forms and finite plastic deformations occur in the direction of internal forces (Fig. 1a). Neglecting the effect of shear forces, the yield conditions for plane frame systems can be expressed in a general form by Eq. (1).

$$K(M, N) = 0 \tag{1}$$

Where $K(M, N)$ is a non-linear function of bending moment $M$ and axial forces $N$.

Geometrical representation of yield condition for a typical RC section is shown Fig. 1(a). In the proposed method, the yield curves representing the yield conditions are idealized as linear segments in order to determine the load increment needed for formation of each plastic section directly. In this case, yield condition is expressed by linear Eq. (2).

$$K(M, N) \cong a_1 M + a_2 N + b = 0 \tag{2}$$

Where $a_1$, $a_2$ and $b$ are the constants that depend on the material and cross-sectional characteristics.

Geometrical representation of linearized yield condition for the same typical RC section is shown in Fig. 1(b). Depending on desired susceptibility, idealization of yield curves can be made by line segments in sufficient number. Yield surfaces for 3-dimensined systems can also be idealized by using plane segments (Irtem 1991, Girgin 1996).

In a plastic section, internal forces are not allowed to violate the yield conditions. This property can be stated as

$$dK = \frac{\partial K}{\partial M}dM + \frac{\partial K}{\partial N}dN = 0 \tag{3}$$

Where $\partial K/\partial M$ and $\partial K/\partial N$ are partial derivatives of the function $K(M, N)$ with respect to $M$ and $N$, respectively.

At the state of bending combined with axial force, plastic deformations that develop in the plastic

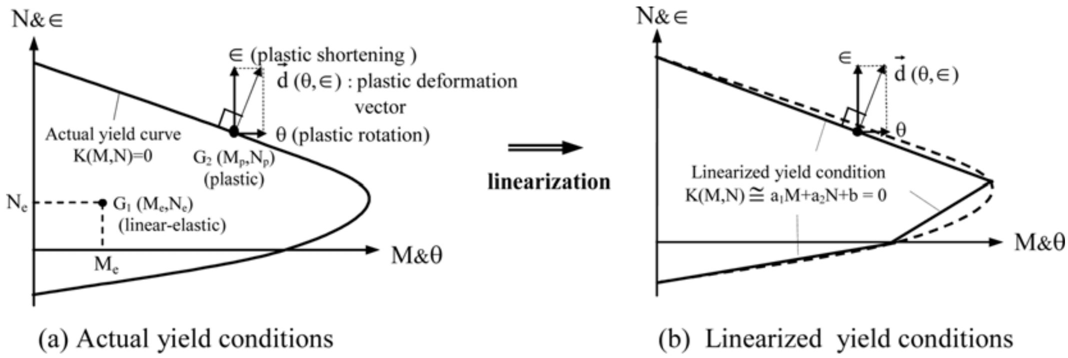


Fig. 1 Yield conditions and plastic deformation vector for a typical RC section

sections are defined by the yield vector $\vec{d}(\theta,\in)$ in which $\theta$ (plastic rotation) and $\in$ (plastic shortening or elongation) are the plastic deformation components in the direction of $M$ and $N$ respectively.

It is known that the yield vector is normal to the yield curve (line) in the sections that have *elastic-perfectly plastic* behavior and homogenous material (Hodge 1959, Cakıroglu and Ozer 1980). Moreover, normality condition is also valid for RC sections in the effect of bending combined with axial force under certain circumstances (Cakıroglu *et al.* 1999). Since the yield vector is assumed to be normal to the yield curve (line), the plastic deformation components may be expressed in terms of a single parameter, as in the following

$$\theta = \phi\frac{\partial K}{\partial M} \qquad \in\, = \phi\frac{\partial K}{\partial N} \tag{4}$$

The parameter $\phi$ is called as the plastic deformation parameter. For idealized yield conditions, the yield condition expressed by Eq. (3) becomes following as

$$\Delta K = a_1\Delta M + a_2\Delta N = 0 \tag{5}$$

Where $\Delta M$ and $\Delta N$ are the bending moment and axial force increments for the related load increment, respectively. In this case, $\theta$ and $\in$ plastic deformation components can be expressed by Eq. (6).

$$\theta = \phi\frac{\partial K}{\partial M} = \phi a_1 \qquad \in\, = \phi\frac{\partial K}{\partial N} = \phi a_2 \tag{6}$$

### 2.3 Determination of unit modal lateral load distributions

The proposed procedure in this study is based on application of incremental response spectrum analyses, which is based on elastic spectral acceleration, proposed by Gupta and Kunnath (2000). However, a new approach different from Gupta and Kunnath (2000) is proposed for the determination of modal lateral loads. In this new approach, modal lateral loads in any load step ($k$) are obtained by adding modal lateral loads comprised of modal properties of system with $k$ plastic sections and modal lateral loads in previous step ($k-1$) (Eq. (7)). Thus, modal lateral loads at any load increment include also the effect of modal lateral loads at the previous load increments. Modal properties and spectral accelerations used in the determination of modal loads vary depending on plastification in the system. Thus, the change of modal effectiveness due to earthquake properties and period elongation can be considered in the analysis. This can be expressed as

$$F_{ij}^{k} = F_{ij}^{k-1} + (\Gamma_j^k \cdot \Phi_{ij}^k \cdot m_i \cdot Sa_j^k) \tag{7}$$

Where $k$ is the number of load increment step, $F_{ij}^{k}$ is the story force $i$ at the mode $j$, $\Gamma_j^k$ is the modal participation factor for $j$th mode, $m_i$ is the mass of $i$th story, $\Phi_{ij}^k$ is the mode shape value at $i$th level and $j$th mode, $Sa_j^k$ is the spectral acceleration for $j$th mode. $Sa_j^k$ is obtained from the considered earthquake spectra depending on the damping ratio ($\xi$) and the instantaneous period for $j$th mode.

At the begining of each load increment, modal properties of the system with plastic sections are determined by free vibration analysis of the system and modal lateral load distribution is calculated. In the study, massless degrees of freedoms (except for freedom of lateral displacement) are condensed for reduction of computation processes and Jacobi iteration is used for free vibration analysis (Bathe 1996).

### 2.4 Non-linear analysis of system with plastic sections for unit load increment

In the proposed multi modal adaptive load increment method, the procedure developed by Ozer (1987), Irtem (1991) and Girgin (1996) was utilized for non-linear analysis of system with plastic sections due to unit load increment, and this procedure is summarized in the following.

#### 2.4.1 Equilibrium equations

After formation of each plastic section, changing stiffness of the system is expressed by adding a new equation defining yield condition in the plastic section to the set of equations. A new unknown in the added equation states $\phi$ plastic deformation parameters defining plastic deformations ($\theta$ and $\in$) in the plastic section (see Eq. (6)). Added equations express that the internal forces in the plastic sections remain on the yield curve (line) during the load increment. Thus, interaction between bending and axial deformations can be considered in the plastic sections subjected to bending combined with axial force during the analysis. Traditional Matrix Displacement (Stiffness) Methods (McGuire *et al.* 2000) are utilized for constitution of equilibrium equations of system with $m$ plastic sections. In these methods, making necessary modifications to account for the plastic sections, the unknowns are considered to be composed of two groups:

a) The components of nodal point displacements, which are called as independent nodal displacements. There are two linear and one rotational displacement at each nodal point for a plane structure.

b) Plastic deformation parameters ($\phi$) representing finite plastic deformations in the plastic sections (See Eq. (6)).

The equations are also considered in two groups:

a) Equilibrium equations of nodes in the direction of the independent nodal displacements.

b) Incremental yield conditions of the plastic sections given by Eq. (5).

Referring to system coordinates, the equilibrium equations of nodes can be expressed by Eq. (8) in matrix form.

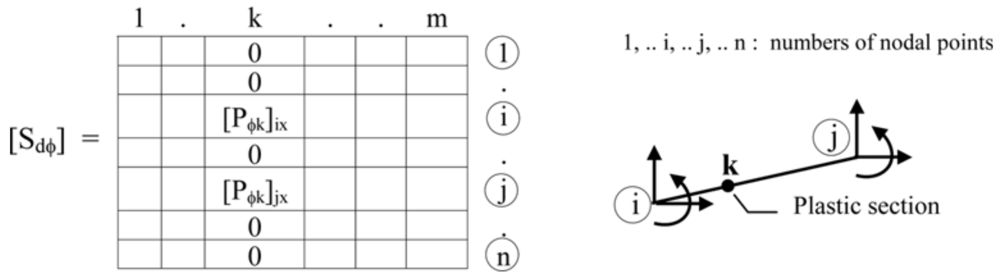


Fig. 2 Derivation of the matrix $[S_{d\phi}]$

$$[S_{dd}][d] + [S_{d\phi}]\,[\phi] + [P_o] = [q] \tag{8}$$

Where;

$[d]$ is the matrix of independent nodal displacements.

$[P_o]$ is the matrix of fixed-end forces due to external load acting between nodes.

$[q]$ is the matrix of nodal external loads.

$[S_{dd}]$ is the elastic stiffness matrix of system. Obtaining this matrix is the same as given in conventional matrix structural analysis books. However, the stability functions including the effect of axial force in the column elements due to gravity loads are taken into account in the determination of elements of matrix $[S_{dd}]$ in order to consider the second order effects.

$[\phi]$ is the matrix of plastic deformation parameters representing plastic deformations in the plastic sections. If the number of plastic section is designated by $m$, this matrix is expressed by Eq. (9).

$$[\phi]^T = [\phi^1 \ldots \phi^k \ldots \phi^m] \;\; (1, ..k, ..m\text{: numbers of plastic sections}) \tag{9}$$

$[S_{d\phi}]$ is a matrix representing the effect of unit plastic deformations in the plastic sections on the equilibrium equations. The size of the matrix $[S_{d\phi}]$ is $(3n \times m)$ for plane systems. A typical column of this matrix consists of the sub matrices $[P_{\phi k}]_{ix}$ and $[P_{\phi k}]_{jx}$ as shown in Fig. 2. These sub matrices in turn, consist of the end-forces (stiffness coefficients) which occur due to unit plastic deformation parameter of $\phi^k = 1$ in the system reference axis. Derivation of the matrices $[P_{\phi k}]_i$ and $[P_{\phi k}]_j$ are summarized in Appendix A.

### *2.4.2 Incremental yield conditions in the plastic sections*

The incremental yield conditions express that the states of internal forces in the plastic sections remain on the yield curve (line) during the load increment. The incremental yield conditions can be expressed by Eq. (10) in the matrix form as

$$[S_{\phi d}]\,[d] + [S_{\phi\phi}]\,[\phi] + [P_{\phi o}] = [0] \tag{10}$$

Here;

$[S_{\phi d}]$ is a matrix representing the effect of internal forces, which occurred in the plastic sections due to unit nodal displacements, on yield conditions. Size of this matrix is $(m \times 3n)$ for a system with $m$ plastic sections. A typical column of this matrix consists of the elements which represent the change of internal forces $(a_1\Delta M + a_2\Delta N)$ occurred in plastic sections due to unit displacement component. It can be proved by the *Betti's reciprocal theorem* that, as long as the plastic deformation vector is normal to the yield curve (line), the matrix $[S_{\phi d}]$ is equal to the transpose of matrix $[S_{d\phi}]$, i.e., $[S_{\phi d}] = [S_{d\phi}]^T$. Therefore derivation of matrix $[S_{\phi d}]$ is not separately needed, considering assumptions adopted in the method.

$[S_{\phi\phi}]$ is a matrix representing the effect of internal forces, which occurred in the plastic sections due to unit plastic deformations, on yield conditions. Size of this matrix is $(m \times m)$ for system with $m$ plastic sections. A typical column of this matrix consists of the elements which represent the change of internal forces $(a_1\Delta M + a_2\Delta N)$ occurred in plastic sections due to unit plastic deformations. Derivations of the elements of this matrix are shown in the Appendix A.

$[P_{\phi o}]$ is a matrix representing effect of internal forces, which occurred in the plastic sections due to external loads, on yield conditions. Size of this matrix is $(m \times 1)$ for system with $m$ plastic sections. A typical column of this matrix consists of the elements which represent the change of internal forces $(a_1\Delta M + a_2\Delta N)$ occurred in plastic sections due to external loads acting between the nodes. Since the lateral loads representing earthquake inertial effects are assumed to act at the nodal points of the system, the matrix $[P_{\phi o}]$ is zero matrix.

When Eqs. (8) and (10) are written together, set of expanded linear equations expressed by Eq. (11) is obtained for the system with plastic sections. The size of the set of expanded equations is $(3n + m) \times (3n + m)$ for plane frame system with $m$ plastic sections. In addition, expanded stiffness matrix is symmetric with respect to its main diagonal of the matrix.

$$\begin{bmatrix} [S_{dd}] & [S_{d\phi}] \\ [S_{\phi d}] & [S_{\phi\phi}] \end{bmatrix} \begin{bmatrix} [d] \\ [\phi] \end{bmatrix} + \begin{bmatrix} [P_o] \\ [P_{\phi o}] \end{bmatrix} = \begin{bmatrix} [q] \\ [0] \end{bmatrix} \tag{11}$$

In the method, elimination of the newly added column, row and nodal loading matrices (modal lateral loads) are sufficient for the solution of this set of equations in any step since the set of the expanded equations in the previous step is already eliminated. Thus, nodal displacement components, $[d]$ and plastic deformation parameters, $[\phi]$ due to unit load increment are effectively obtained for multi-mode.

After determination of unknowns (matrices $[d]$ and $[\phi]$) for unit load increment, end-forces (matrices $[P]_{ix}$ and $[P]_{jx}$) of the elements with plastic sections are obtained by Eq. (12) in matrix form. Then, these end-forces matrices at the system reference axis are transformed to the local axis of the elements by related transforming matrices. The terms of $([P_\phi]_{ix}\,[\phi]_{ij})$ and $[P_\phi]_{jx}\,[\phi]_{ij})$ in the Eq. (12) are omitted for the elements without any plastic sections.

$$\begin{aligned} [P]_{ix} &= [k]_{ixix}\,[d]_{ix} + [k]_{ixjx}\,[d]_{jx} + [P_o]_{ix} + [P_\phi]_{ix}\,[\phi]_{ij} \\ [P]_{jx} &= [k]_{jxix}\,[d]_{ix} + [k]_{jxjx}\,[d]_{jx} + [P_o]_{jx} + [P_\phi]_{jx}\,[\phi]_{ij} \end{aligned} \tag{12}$$

Where $[k]_{ixix}$, ..... $[k]_{jxjx}$ are the individual element stiffness matrices transformed to the system (global) reference axis, $[d]_{ix}$ and $[d]_{jx}$ are matrices of independent nodal displacements at the nodes $i$ and $j$, $[P_\phi]_{ix}$ and $[P_\phi]_{jx}$ are matrices composed of the end forces due to the unit plastic deformation ($\phi^k = 1$) of the plastic section on element $ij$, $[\phi]_{ij}$ is a column matrix consisting of plastic deformations of the plastic section on element $ij$, $[P_o]_{ix}$ and $[P_o]_{jx}$ are matrices of fixed-end forces at nodes $i$ and $j$.

### 2.5 Determination of the response quantities for unit load increment

In the proposed method, modal response quantities ($R_j^k$), which are obtained independently for each modal distribution, are combined by an appropriate combination rule, as in the traditional response spectrum analysis. Thus, combined response quantities ($\Delta R_C^k$) occurred due to unit load increment, which include the interaction of all modes, are obtained. When combining the response quantities, either the rules of Square Root of Sum of Squares (SRSS) or the rules of Complete Quadratic Combination (CQC) are used depending on the nearness of modal periods (Chopra 2001). Signs of the combined response quantities are always positive at the end of the combination. However, sign of the internal forces (bending moments and axial forces) should be considered in determination of plastic sections by using yield conditions. Therefore, using of sign of the effective mode in the related load increment step was adopted for sign of combined quantities in this study.

### 2.6 Determination of plastic section and related response quantities

Location of any plastic section called ($k$) and related lateral load increment are determined by using the yield conditions of potential (critical) plastic sections. Therefore, Eq. (13) is used in the sections subjected to bending moment only (i.e., beam element), while Eq. (14) is used in the sections subjected to bending moment combined with axial force (i.e., column element).

$$K(M) = M^{k-1} + \Delta P^k \Delta M_C^k - M_p = 0 \tag{13}$$

$$K(M, N) = a_1(M^{k-1} + \Delta P^k \Delta M_C^k) + a_2(N^{k-1} + \Delta P^k \Delta N_C^k) + b = 0 \tag{14}$$

Where $k$ is number of load increment step, $\Delta P^k$ is load increment factor for the related section, $M_p$ is the bending moment capacity of the related section, $M^{k-1}$ and $N^{k-1}$ are, respectively, the bending moment and axial force in the related section in previous step. $M^{k-1}$ and $N^{k-1}$ state the bending moment and the axial force due to the gravity loads in the first load increment step. $\Delta M_C^k$ and $\Delta N_C^k$ are, respectively, the combined bending moment and combined axial force in the related section due to unit load increment.

$\Delta P^k$ load increment factors for all potential plastic sections in the system are calculated and then the minimum load increment factor $\Delta P_{\min}^k$ is determined. Thus, location of plastic sections in the load increment step $k$ and the corresponding load increment factor are determined. Then, required response quantities ($R^k$) (nodal displacement, story drift, plastic rotation etc.) belonging to the load increment step $k$ are obtained by Eq. (15).

$$R^k = R^{k-1} + \Delta P_{\min}^k \Delta R_C^k \tag{15}$$

### 2.7 Summary of analysis steps of the method

Analysis steps of the proposed method are summarized below.

1) Determine the moment-curvature relationships of all elements and actual yield conditions of columns by using the material and cross-section properties of the elements. Idealize the moment-curvature relationships as elastic-perfectly plastic. Idealize the yield conditions by using line segments in sufficient numbers for the required accuracy level.

2) Determine the response quantities (internal forces, nodal displacements etc.) for gravity loads. Considering the effects of the axial forces on element stability functions, obtain the system stiffness matrix including the second order effects. Check whether any plastic section occurs in the system due to gravity loads or not. Repeat the processes explained in steps 6 and 7 for gravity load increments until required gravity load level is reached in case any plastic section occurs. Then start the processes for modal lateral load increment.

3) Condense the system stiffness matrix for required degree of freedoms and obtain dynamic stiffness matrix. Perform free vibration analysis, determine the modal properties of the system with plastic sections and then determine modal lateral load distribution using Eq. (7) for considered modes.

4) Obtain unit modal response quantities ($[d]$, $[\phi]$ etc.) for each modal load distribution independently. For this purpose, utilize from the eliminated system stiffness matrix in the previous step.

5) Determine the combined response quantities ($\Delta R_C^k$) due to unit load increment by using appropriate modal combination rule. Assign the sign of effective mode in the current step to the combined response quantities for usage at the yield conditions.

6) Determine the location of plastic section and related load increment factor ($\Delta P_{\min}^k$) in the current step by using yield conditions in all potential plastic sections. Then obtain the response quantities in the current step by using Eq. (15).

7) Add the $\phi^k$ plastic deformation parameter representing plastic deformations in the plastic section to the current unknowns as a new unknown. Obtain the set of expanded equations, by adding the matrices of $[S_{d\phi}]$, $[S_{\phi d}]$, $[S_{\phi\phi}]$ and $[P_{\phi o}]$ to the current set of equations.

8) Repeat the process (starting from step 3) until the limit state of instability of the system. When the system reaches this limit state, the determinant of the expanded stiffness matrix of the system is negative or zero, that is, the expanded stiffness matrix loses its positive definite attribute.

## 3. Evaluation of the proposed method

The proposed method was evaluated by taking the results of Non-linear Dynamic Analysis (NDA) as reference (accurate solution). In addition, the proposed method was compared with FEMA 356 Non-linear Static Analysis (NSA) procedures (FEMA 2000) using fixed loads distributions (first mode, SRSS and uniform distribution) and the effectiveness of the method was shown. Considered parameters in the evaluation study are floor displacements, story drifts, max. beam plastic rotations, story shears, capacity curves (displacement and base shear demands) and distribution of plastic sections in the system.

### 3.1 Properties of structural model and ground motions

The evaluation study was carried out on a 20-story building, which is affected by higher modes. Geometrical properties of the building are shown in Fig. 3. Seismic design of the building was based on Turkish Earthquake Code (TEC 1998). The building was designed according to high ductility level ($R = 8$), seismic zone of 1, and importance factor of 1. An internal frame of the building (axis of B-B) was considered for the evaluation in this study. The element details of the considered frame are presented in Table 1. Each story mass of the frame is 72.9 kNs$^2$/m. First mode period, $T_1$ of the frame with effective (cracked section) stiffness is found to be 3.49s. Additional detailed information about the building can be found in the dissertation prepared by Turker (2005).

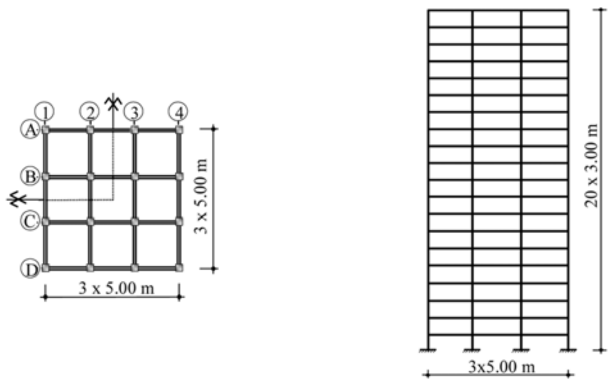


(a) Typical plan of the building (b) Elevation of the building (axis B-B)

Fig. 3 Geometrical properties of the building

Table 1 Element details of the frame

| Story | Place | Steel of beams ($cm^2$) Support (1), (2) | Steel of beams ($cm^2$) Span (1-2), (2-3) | Size of beams (cm*cm) |
|---|---|---|---|---|
| **1** | top | 9.43 | 6.28 | 30*70 |
| | bottom | 6.28 | 6.28 | |
| **2-8** | top | 12.57 | 6.28 | |
| | bottom | 9.43 | 6.28 | |
| **9-14** | top | 12.57 | 6.28 | 30*60 |
| | bottom | 9.43 | 6.28 | |
| **15-16** | top | 9.43 | 6.28 | |
| | bottom | 6.28 | 6.28 | |
| **17-19** | top | 9.43 | 6.28 | 25*50 |
| | bottom | 6.28 | 6.28 | |
| **20** | top | 6.28 | 6.28 | |
| | bottom | 6.28 | 6.28 | |
| Story | Name | Steels of columns ($cm^2$) | Size of columns (cm*cm) | |
| **1-4** | B1,B4 | 54.24 | 70*70 | |
| | B2,B3 | 72.32 | 80*80 | |
| **5-8** | B1,B4 | 37.68 | 60*60 | |
| | B2,B3 | 50.24 | 70*70 | |
| **9-12** | B1,B4 | 25.12 | 50*50 | |
| | B2,B3 | 37.68 | 60*60 | |
| **13-16** | B1,B4 | 18.48 | 40*40 | |
| | B2,B3 | 25.12 | 50*50 | |
| **17-20** | B1,B4 | 13.56 | 35*35 | |
| | B2,B3 | 18.80 | 40*40 | |

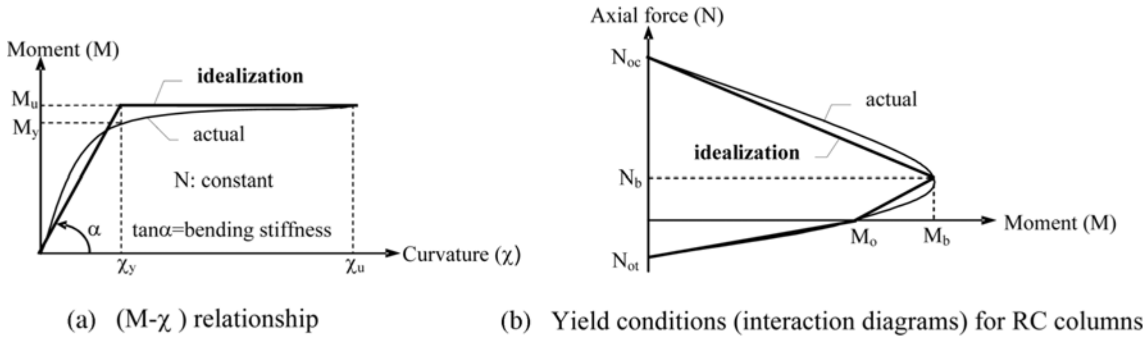


Fig. 4 Idealization of behaviors of RC elements

To apply the proposed method to RC buildings, behavior of RC sections should be idealized according to the principles of the method. For this purpose, the moment-curvature ($M-\chi$) relationships, which were determined by using the material and section properties, of the elements were idealized as shown in Fig. 4(a). Actual yield conditions of the columns with symmetric section were idealized by three line segments as shown in Fig. 4(b). Similar characteristic values ($M_o$, $M_b$, $N_{ot}$, $N_{oc}$, $N_b$) can also be used for the idealizations of non-symmetric sections.

As shown in Fig. 4(a), $M_y$ is the yielding moment of section, $M_u$ is the moment bearing capacity of section under constant axial force, $\chi_y$ and $\chi_u$ are the yielding curvature and ultimate (failure) curvature of the section, respectively. At the graphics shown in Fig. 6(b), $N_{ot}$, $N_{oc}$ and $N_b$ are axial load capacity of the section in tension, compression and at balanced failure, respectively. $M_o$ and $M_b$ are the moment bearing capacity of the section in pure bending and that at balanced failure, respectively.

As shown in Fig. 1(a), initial stiffness on the idealized moment-curvature relationship was used for beam and column elements. Depending on the reinforcement included, beams were defined as having two support region and one span region. Lengths of these regions were accepted as equal. Bending stiffness belonging to bending moment due to gravity loads was used at the each region of the beams. Axial forces due to gravity loads were considered in determination of bending stiffness of columns. These section properties were generated by using a special-purpose program (BEKE-3, by Girgin 1996).

In the evaluation of the proposed method, three ground motions that have different frequency content were used (PEER 2005) (Table 2). Acceleration records and spectrums, with 5% damping, of these ground motions are presented Fig. 5.

Table 2 Properties of the earthquakes

| Earthquake | Component | Magnitude (M) | Peak ground aceleration (g) | Peak ground velocity (cm/s) | Peak ground dispalcement (cm) |
|---|---|---|---|---|---|
| Imperial Valley-USD (1940) | ELC-180 | 7.0 | 0.313 | 29.8 | 13.32 |
| Erzincan-Turkey (1992) | ERZ-DB | 6.9 | 0.496 | 64.3 | 22.78 |
| Kocaeli-Turkey (1999) | SKR-090 | 7.4 | 0.376 | 79.5 | 70.52 |

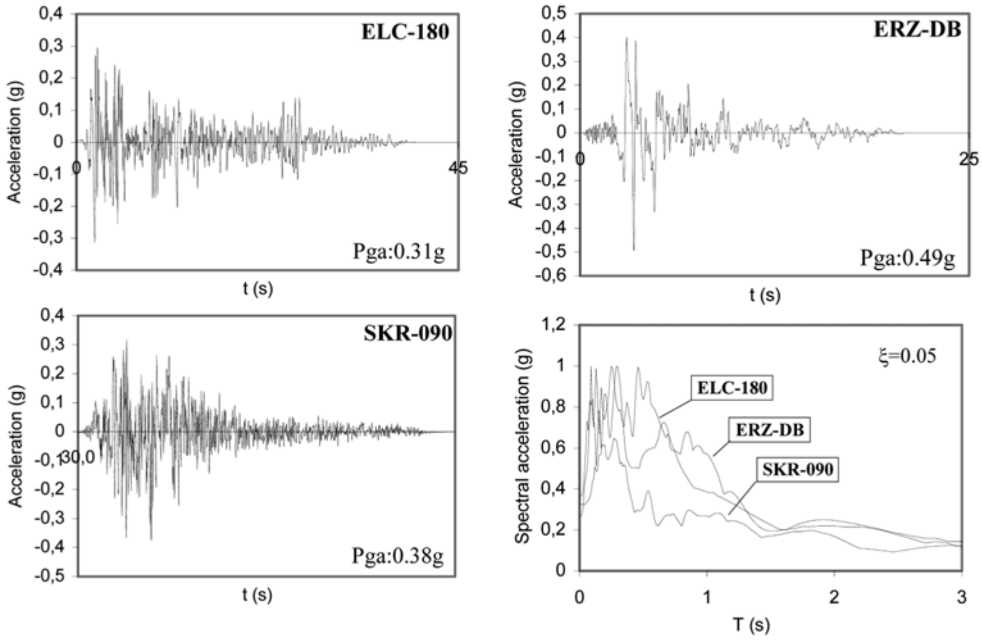


Fig. 5 Acceleration records and spectrums of ground motions used in the evaluation

### *3.2 Properties of the analysis*

In all non-linear analyses, gravity loads composed of (1.0 dead load+1.0 live load) were used. Acceleration spectrums obtained from actual ground motions were used in order to compare the method results with those of the NDA. In the proposed method, all modes of the frame were considered. However, analysis including 1 mode, 2 modes, 3 modes and 4 modes were also carried out separately on the 20 story frame in order to determine the effect of number of mode considered in the analysis and obtained results were compared with each other and the results including all modes. It was seen that consideration of the first three modes was sufficient and effect of other modes could be neglected. Details of these analyses can be found in Turker (2005). Numerical applications of the proposed method were performed by program MEPARCS (Turker 2005).

In the NDA of the frame for different ground motions, stiffness proportional damping was assumed and damping ratio ($\xi$) of 5% was used. *Perfectly rigid plastic* behavior that was compatible with assumptions of NSA was assumed for hysteretic moment-plastic rotation relationship of beam and column elements in the NDAs**.** The program RAM Perform-2D (RAM Int. 2000) was used for the NDAs of the frame.

The proposed method was also evaluated by comparing the obtained results with those of FEMA 356 NSA procedures using fixed loads distributions in order to show the effectiveness of the method. Descriptions of these distributions are summarized below.

a) *First mode distribution:* Forces proportional to the first mode shape are used in this distribution.

b) *SRSS distribution:* Forces proportional to the story shear forces obtained by elastic response spectrum analysis (RSA) are used in this distribution proposed for building affected by higher modes. Therefore, the distribution is called briefly as “SRSS”. In the determination of this distribution, consideration of a sufficient number of modes is stipulated in FEMA 356. In the determination of this distribution, spectral accelerations (Sa) obtained from related ground motions were used and four modes of the frame were considered in the RSA.

c) *Uniform distribution:* Forces proportional to the masses in the each story of frame are used in this distribution.

### 3.3 Comparison and evaluation of the analysis results

Comparisons of the results obtained from the NDA, the proposed method and NSAs for FEMA 356 (2000) procedures were carried out on response quantities obtained in the instability limit state of the proposed method. Therefore, the ground motion records in the NDAs were scaled to obtain the roof displacements occurred at the instability limit state. Maximum response quantities occurred during NDA for related records were taken as reference (accurate value) for comparisons of the results. In addition, “Dynamic Pushover Analysis” approach (Elnashai 2001) was used for the evaluation of the capacity curves (base shear and roof displacement demands). All the response quantities obtained from the proposed method, the NDAs and NSAs procedures in FEMA 356 are presented in Figs. 6-8.

The first mode distribution is independent from the earthquake characteristics. Therefore, this distribution yields the similar characteristic results for the investigated frame for all of the analyses. The higher modes were not very effective in the behavior of the frame due to frequency content of the SKR-090 record. Therefore, it was generally obtained good results from the first mode distribution for all parameters except for the shear forces. However, the story drifts, beam plastic rotations and distribution of plastic sections in the upper stories of the frame due to the higher mode effects of ELC-180 and ERZ-DB records could not be determined by the first mode distribution (Figs. 6-8).

The uniform distribution is also independent from the earthquake characteristics and yields the similar characteristic results in the investigated frame for all analyses. As expected, it was seen that the uniform distribution in FEMA 356 yielded quite different results from other analyses for all response quantities. When the NDA results are taken as reference, it was seen that this distribution yielded very high values for floor displacements in all stories of the frame, very low values for story drift and beam plastic rotations in the upper stories of the frame, very high values for story drift and beam plastic rotations in the lower stories of the frame, very low values for story shears in all stories of the frame (Fig. 6). This distribution yielded better values only for a few story shears than the proposed method and other FEMA 356 distributions (Fig. 7). As seen in Fig. 8, this distribution was also insufficient in the determination of the distribution of plastic sections in the middle and upper stories.

The SRSS distribution includes the earthquake characteristics by using elastic spectral accelerations of the records. Story drifts, beam plastic rotations and distribution of plastic sections in the upper stories of the frame due to higher mode effects at ELC-180 and ERZ-DB records could be determined very well by the SRSS distribution (Figs. 6-8). However, as seen in the figures, the SRSS distribution was insufficient in the determination of the story drifts, beam plastic rotations and distribution of plastic sections in the middle and lower stories of the frame (Figs. 6-8).

The proposed method includes the earthquake characteristics and changing dynamic properties (period elongations and spectral amplifications) of the frame. Therefore, general characteristics

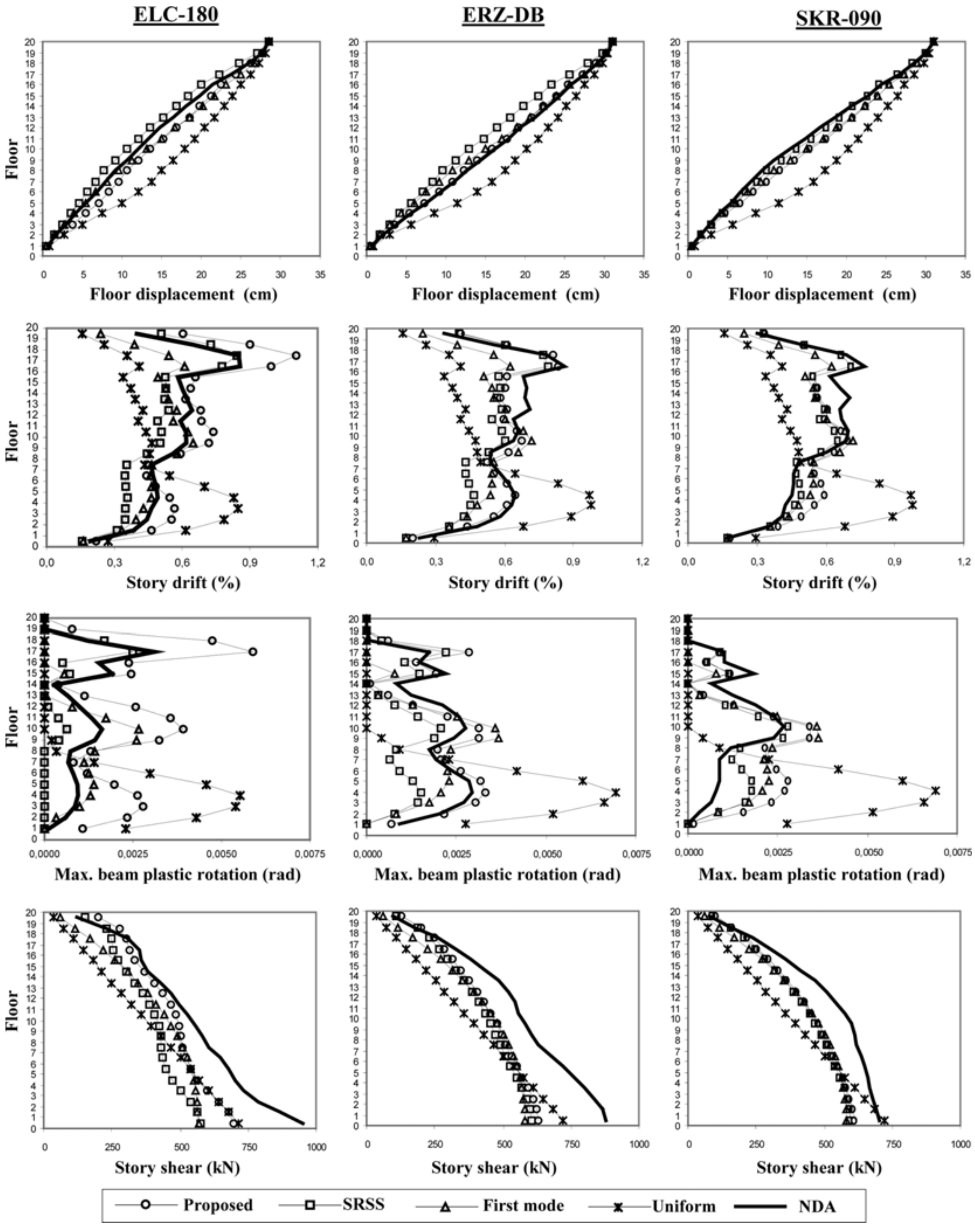


Fig. 6 Comparison of floor displacements, story drifts, max. beam plastic rotations and story shears

predicted by the NDA could be obtained appropriately by the proposed method for almost all the parameters. The proposed method yielded high values for beam plastic rotations in some stories of the frame for ELC-090 records only. In addition, it yielded generally low values for story shears in

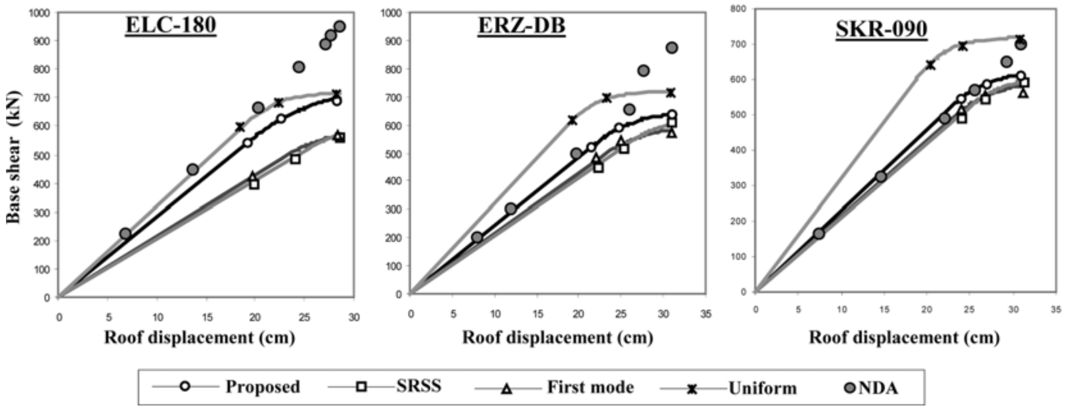


Fig. 7 Comparison of capacity curves of the system

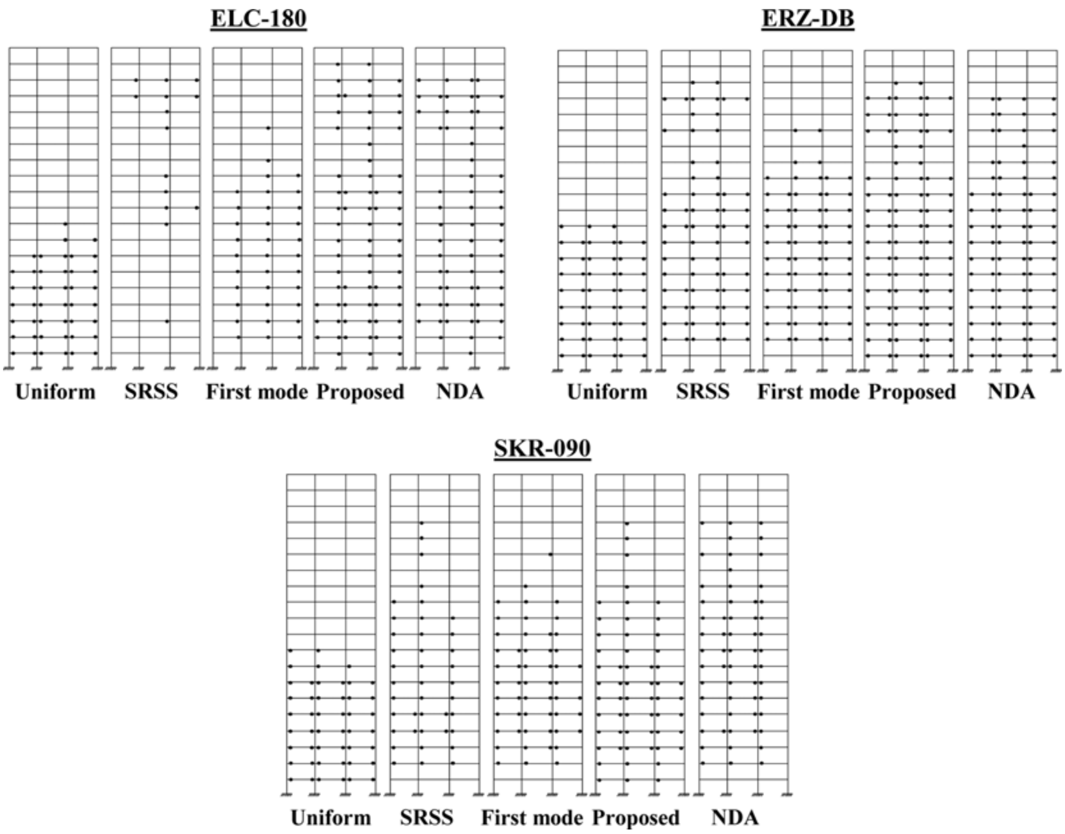


Fig. 8 Comparison of distribution of plastic sections in the system

the lower stories of the frame and capacity curves (base shear and roof displacement demands). However, these results are better than those of all FEMA 356 procedures owing to the contribution of higher modes. Consequently, it can be seen that, the proposed method yielded generally better results than all FEMA 356 procedures for all of the investigated parameters.

More detailed evaluation study including different regular RC buildings, which represent a broad period range, were carried out in the dissertation prepared by Turker (2005). In that study, very similar results were also obtained for structures with wide range of period.

### 3.4 Investigation of second order effects

In the proposed method, the analysis neglecting the second order effects (first order only) was carried out in order to determine the effectiveness of the second order effects on the response quantities and periods of the system and then the obtained results were compared with the analysis results considering the second order effects. Similar results were obtained for each earthquake record. As an example, the results obtained for ERZ-DB records were presented in this study (Fig. 9).

It was found that the story drifts and beam plastic rotations increased in the lower stories of the frame and decreased in the upper stories of the frame due to consideration of the second order effects (Fig. 9). The story shears and base shear capacity of the frame also decreased owing to the

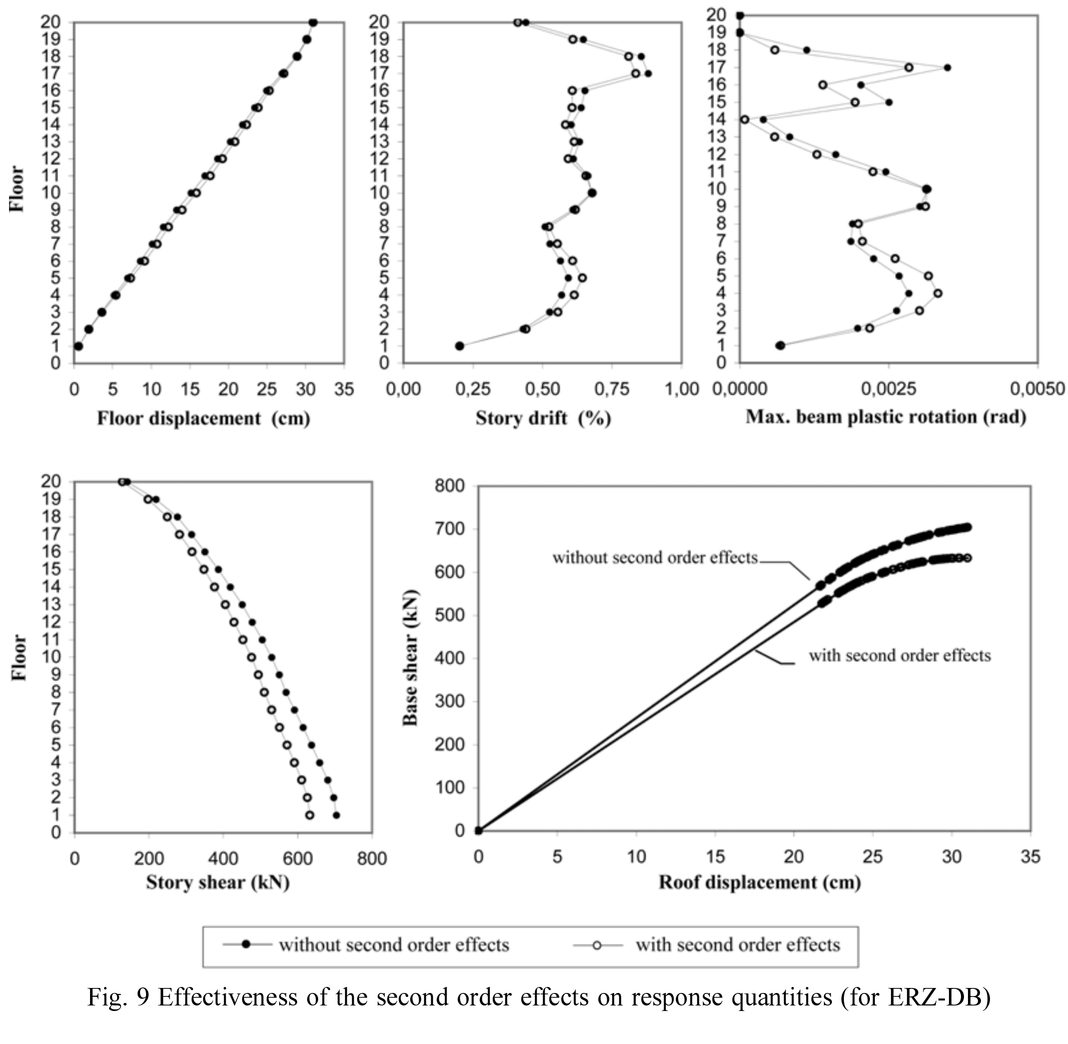


Fig. 9 Effectiveness of the second order effects on response quantities (for ERZ-DB)

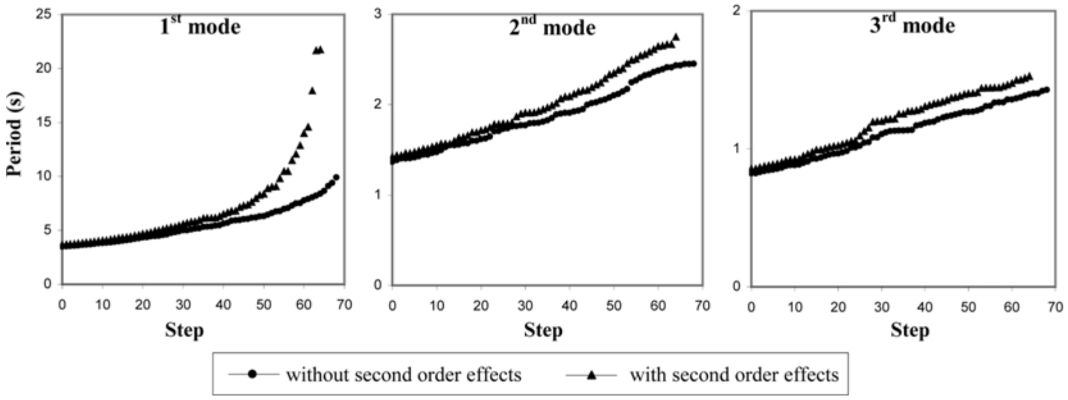


Fig. 10 Effectiveness of the second order effects on first three periods of the system

second order effects as expected (Fig. 9). Change of the floor displacements and the distributions of plastic sections in the system due to the second order effects were very small.

In the proposed method, the second order effects are also considered in the determination of modal properties of system. Modal periods of the system enlarged due to the second order effects as expected (Fig. 10). When the plastification in the system is increased, effectiveness of second order effects also increased and large increments occurred especially on the first mode period (Fig. 10).

## 4. Conclusions

An effective load increment method is presented for multi-mode adaptive non-linear static analysis of buildings. Lumped plastisicity approach is adopted and geometrical non-linearties (second-order effects) are included in the method. Geometrical non-linearity effects and yield conditions of column elements are linearized. Thus, load increments for formation of plastic sections can be determined directly (without iteration or using a step-by-step solution) by using linearized yield conditions. Formation of all plastic sections and the changing modal properties of the system due to plastification can be determined in detail in the proposed method.

Different scaling approximations can be used in each step for calculating the modal lateral loads because of using unit lateral load increment in the method. When the second order effects are neglected in the analysis, the distribution of response quantities change considerably along the building height. Furthermore, it is seen that modal periods of system change also considerably (particularly for the first mode period) with increasing plastification due to the second order effects.

End of the evaluations when NDA results are taken as reference, the proposed method yields generally better results than all FEMA 356 procedures (first mode, SRSS, uniform) for all the investigated parameters (floor displacements, story drifts, max. beam plastic rotations, story shears, capacity curves and distribution of plastic sections). First mode distribution in FEMA 356 yields generally good results in the lower stories, but it is not sufficient for determination of the response quantities in the upper stories. SRSS distribution proposed in FEMA 356 to consider higher mode effects, yields generally good results in the upper stories, but it is not sufficient for determination of the response quantities in the middle and lower stories of the frame. Uniform distribution in FEMA

356 is generally not sufficient for determination of the response quantities in all stories of the frame.

In conclusion, the proposed method is generally found compatible with NDA. Furthermore, it yields better results than all NSA procedures proposed by FEMA 356. However, the proposed procedure should further be evaluated through statistical studies considering various regular and irregular buildings and ground motion records. Therefore, the authors are continuing to the studies in this subject.

## References

Antoniou, S., Rovithakis, A. and Pinho, R. (2002), "Development and verification of a fully adaptive pushover procedure", *12th European Conf. on Earthquake Engineering*, London.

Aschheim, M.A. and Hernandez-Montes, E. (2006), "Observations on the reliability of alternative multiple-mode pushover analysis methods", *J. Struct. Eng.*, **132**, 471-477.

Aydınoğlu, M.N. (2003), "An incremental response spectrum analysis procedure based on inelastic spectral displacements for multi-mode seismic performance evaluation", *Bulletin of Earthq. Eng.*, **1**, 3-36.

Bathe, J.K. (1996), *Finite Element Procedures*, Prentice Hall, Englewood Cliffs, New Jersey.

Chopra, A.K. and Goel, R.K. (2001), "A modal pushover analysis procedure to estimate seismic demands for buildings: Theory and preliminary evaluation", Pasific Earthquake Engineering Research Center (PEER), Report No. 2001/03, University of California, Berkeley, California.

Chopra, K.A. (2001), *Dynamics of Structures*, Second Edition, Prentice Hall, New Jersey.

Chopra, A.K. and Goel, R.K. (2002), "A modal pushover analysis procedure for estimating seismic demands for buildings", *Earthq. Eng. Struct. Dyn.*, **31**, 561-582.

Çakıroğlu, A. and Özer, E. (1980), *Materially and Geometrically Non-Linear Systems*, Vol. 1 (in Turkish), Istanbul Technical University Publications, Istanbul.

Çakıroğlu, A., Özer, E. and Girgin, K. (1999), "Yield conditions and yield vector for combined biaxial bending of rectangular reinforced concrete sections", *Proc. of the Uğur Ersoy Symposium on Structural Engineering*, Ankara.

Elnashai, A.S. (2001), "Advanced inelastic static (pushover) analysis for earthquake applications", *Struct. Eng. Mech.*, **12**, 51-69.

FEMA (2000), *Prestandard and Commentary for the Seismic Rehabilitation of Buildings*, FEMA 356, American Society of Civil Engineers, Virginia.

FEMA (2004), *Improvement of Nonlinear Static Seismic Analysis Procedures*, FEMA 440 (ATC-55 project), Federal Emergency Management Agency, Washington, D.C.

Girgin, K. (1996), "A method of load increments for the determination of second-order limit load and collapse safety of reinforced concrete framed structures", Ph.D. Thesis, Istanbul Technical University, Institute of Science, Istanbul.

Goel, R.K. and Chopra, A.K. (2005), "Role of higher - "Mode" Pushover analyses in seismic analysis of buildings", *Earthquake Spectra*, **21**, 1027-1041.

Gupta, B. and Kunnath, S.K. (2000), "Adaptive spectra-based pushover procedure for seismic evaluation of structures", *Earthquake Spectra*, **16**, 367-391.

Hernandez-Montes, E., Kwon, O.-S. and Aschheim, M.A. (2004), "An energy-based formulation for first-and multiple-mode nonlinear static (Pushover) analyses", *J. Earthq. Eng.*, **8**, 69-88.

Hodge, P.G. (1959), *Plastic Analysis of Structures*, Mc. Graw Hill.

İrtem, E. (1991), "Determination of second-order limit load of framed space structures by a method of load increment", Ph.D. Thesis, Istanbul Technical University, Institute of Science, Istanbul.

Jan, T.S., Liu, M.W. and Kao, Y.C. (2004), "An upper-bound pushover analysis procedure for estimating the seismic demands of high-rise buildings", *Eng. Struct.*, **26**, 117-128.

Kim, S. and D'Amore, E. (1999), "Push-over analysis procedure in earthquake engineering", *Earthquake Spectra*, **15**, 417-434.

Lawson, R.S., Vance, V. and Krawinkler, H. (1994), "Nonlinear static push-over analysis-why, when, and how?",

*Proc. of Fifth U.S. Nat. Conf. on Earthquake Engineering*, **1**, 283-292, Chicago.
McGuire, W., Gallagher, R.H. and Ziemian, R.D. (2000), *Matrix Structural Analysis*, 2nd Edition, John Wiley.
Moghadam, A.S. (1998), "A pushover procedure for tall buildings", *Proc. of 12th European Conf. on Earthquake Engineering,* Balkema, Rotterdam, London.
Mwafy, A.M. and Elnashai, A.S. (2001), "Static pushover versus dynamic collapse analysis of RC buildings", *Eng. Struct.*, **23**, 407-424.
Özer, E. (1987), "Determination of the second-order limit load by a method of load increments", *Bulletins of the Technical University of Istanbul*, **40**, 815-835.
Paret, T.F., Sasaki, K.K., Eilbeck, D.H. and Freeman, S.A. (1996), "Approximate inelastic procedures to identify failure mechanisms from higher mode effects", *Proc. of Eleventh World Conf. on Earthquake Engineering*, Acapulco, Mexico.
Pacific Earthquake Engineering Research Center. (PEER) (2005), Strong Motion Database, http://www.peer.berkeley.edu.
RAM International. (2004), RAM Perform-2D User guide and element descriptions, Version 1.30, http://www.ramint.com.
Rovithakis, A. (2001), "Verification of adaptive pushover analysis procedures", M.Sc. Thesis, Imperial College of Science, Technology and Medicine, U.K.
TEC (1998), *Turkish Earthquake Code*, The Minister of Public Works and Settelement, Ankara.
Türker, K. (2005), "Multi modal adaptive load increment method for determination of earthquake response of structures", Ph.D. Thesis, Balıkesir University, Institute of Science, Balıkesir.
Yang, P. and Wang, Y. (1998), "A study on improvement of pushover analysis", *Proc. of 12th World Conf. on Earthquake Engineering*, Auckland, New Zealand.

## Appendix A

1) Derivation of end forces due to unit plastic deformation parameters in the plastic section
As shown in Fig. A1, end forces due to unit plastic deformation parameters in the plastic section are obtained from combination of end forces occurred at four different deformation states.

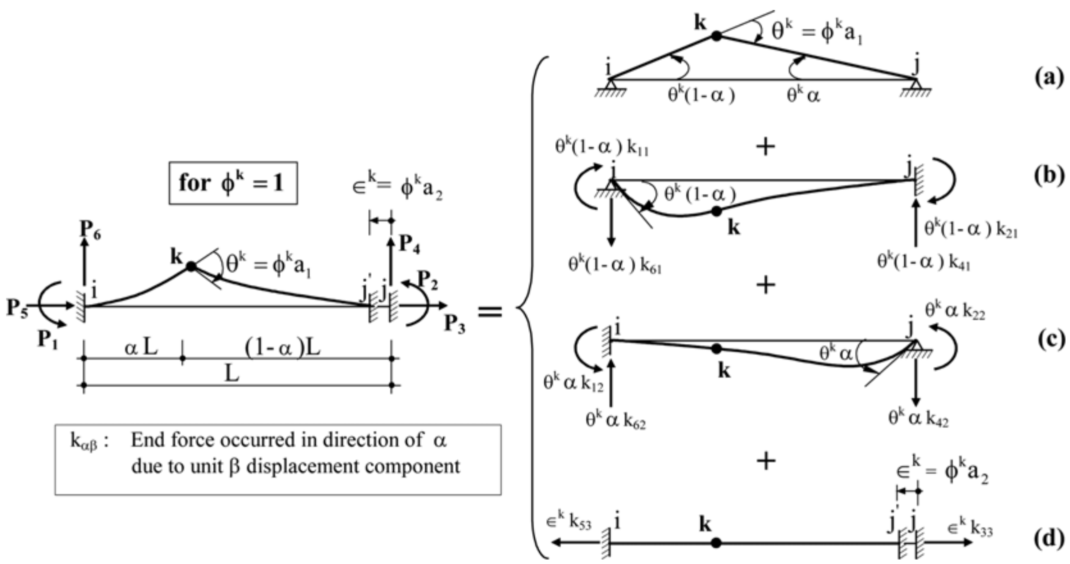


Fig. A1 Derivation of end-forces due to unit plastic deformation parameters

Matrices of $[P_{\phi k}]_i$ and $[P_{\phi k}]_j$ obtained from superposition of end forces in Fig. A1 are given below.

$$[P_{\phi k}]_i = \begin{bmatrix} P_1 \\ P_5 \\ P_6 \end{bmatrix} = \begin{bmatrix} \theta^k[\alpha k_{12} - (1-\alpha)k_{11}] \\ -\in^k k_{53} \\ \theta^k[\alpha k_{62} - (1-\alpha)k_{61}] \end{bmatrix} \quad [P_{\phi k}]_j = \begin{bmatrix} P_2 \\ P_3 \\ P_4 \end{bmatrix} = \begin{bmatrix} \theta^k[\alpha k_{22} - (1-\alpha)k_{21}] \\ \in^k k_{33} \\ \theta^k[(1-\alpha)k_{41} - \alpha k_{42}] \end{bmatrix} \tag{1}$$

Referring to the individual element coordinates, matrices $[P_{\phi k}]_i$ and $[P_{\phi k}]_j$ for a prismatic element which does not include the second order effects become

$$[P_{\phi k}]_i = \begin{bmatrix} P_1 \\ P_5 \\ P_6 \end{bmatrix} = \begin{bmatrix} \theta^k[(6\alpha-4)EI/L] \\ -\in^k EF/L \\ \theta^k[(12\alpha-6)EI/L^2] \end{bmatrix} \quad [P_{\phi k}]_j = \begin{bmatrix} P_2 \\ P_3 \\ P_4 \end{bmatrix} = \begin{bmatrix} \theta^k[(6\alpha-2)EI/L] \\ \in^k EF/L \\ -\theta^k[(12\alpha-6)EI/L^2] \end{bmatrix} \tag{2}$$

Where $EI$ and $EF$ are the bending stiffness, the axial stiffness, respectively.
Matrices $[P_{\phi k}]_i$ and $[P_{\phi k}]_j$ for a prismatic element including the second order effects become

$$[P_{\phi k}]_i = \begin{bmatrix} P_1 \\ P_5 \\ P_6 \end{bmatrix} = \begin{bmatrix} \theta^k[-(1-\alpha)b_{11} + \alpha b_{12}] \\ -\in^k EF/L \\ \theta^k(2\alpha-1)(b_{11}+b_{12})/L \end{bmatrix} \quad [P_{\phi k}]_j = \begin{bmatrix} P_2 \\ P_3 \\ P_4 \end{bmatrix} = \begin{bmatrix} \theta^k[\alpha b_{11} - (1-\alpha)b_{12}] \\ \in^k EF/L \\ -\theta^k(2\alpha-1)(b_{11}+b_{12})/L \end{bmatrix} \tag{3}$$

Where $b_{11}$, $b_{12}$ are expressed by

$$b_{11} = \frac{EI}{L} \cdot \frac{\varphi\sin\varphi - \varphi^2\cos\varphi}{2(1-\cos\varphi) - \varphi\sin\varphi} \qquad b_{12} = \frac{EI}{L} \cdot \frac{\varphi^2 - \varphi\sin\varphi}{2(1-\cos\varphi) - \varphi\sin\varphi} \tag{4}$$

Where $N$ is the axial force (compression) and $\varphi = L\sqrt{\frac{|N|}{EI}}$.

2) Derivation of $\Delta M$ and $\Delta N$ internal force variation in any section of element with a plastic section
For the element which is not including the second order effects,

$$\Delta M(x) = \frac{x}{L}P_2 - \left(1 - \frac{x}{L}\right)P_1$$

$$\Delta N(x) = P_5 \tag{5}$$

For the element including the second order effects, (for $\alpha = \frac{x_k}{L}$)

$$\text{For } x \le \alpha L \ : \Delta M(x) = \frac{P_2 \cdot \sin\left(\varphi \cdot \frac{x}{L}\right) - P_1 \cdot \sin\left(\varphi \cdot \left(1 - \frac{x}{L}\right)\right)}{\sin\varphi} - |N| \cdot (1-\alpha) \cdot x \cdot \theta^k$$

$$\text{For } x > \alpha L \ : \Delta M(x) = \frac{P_2 \cdot \sin\left(\varphi \cdot \frac{x}{L}\right) - P_1 \cdot \sin\left(\varphi \cdot \left(1 - \frac{x}{L}\right)\right)}{\sin\varphi} - |N| \cdot (L-x) \cdot \alpha \cdot \theta^k$$

$$\text{For } 0 \le x \le L \ : \Delta N(x) = P_5 \tag{6}$$

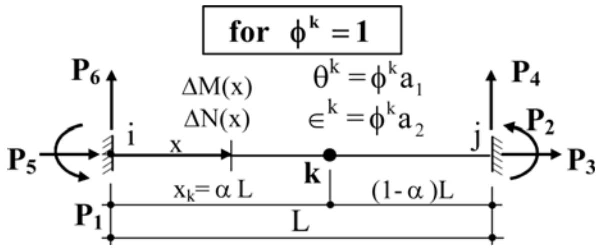


Fig. A2 Variation of the internal forces in the element with a plastic section